

Effect of structural vacancies on lattice vibration, mechanical, electronic, and thermodynamic properties of Cr_5BSi_3

Tian-Hui Dong(董天慧), Xu-Dong Zhang(张旭东), Lin-Mei Yang(杨林梅), and Feng Wang(王峰)
Citation: Chin. Phys. B, 2022, 31 (**2**): 026101. DOI: 10.1088/1674-1056/ac11e2
Journal homepage: http://cpb.iphy.ac.cn; http://iopscience.iop.org/cpb

What follows is a list of articles you may be interested in

Probing structural and electronic properties of divalent metal Mg_{n+1} and $SrMg_n$ (n = 2–12) clusters and their anions

Song-Guo Xi(奚松国), Qing-Yang Li(李青阳), Yan-Fei Hu(胡燕飞), Yu-Quan Yuan(袁玉全), Ya-Ru Zhao(赵亚儒), Jun-Jie Yuan(袁俊杰), Meng-Chun Li(李孟春), and Yu-Jie Yang(杨雨杰)
Chin. Phys. B, 2022, 31 (**1**): 016106. DOI: 10.1088/1674-1056/ac04aa

*t*P40 carbon: A novel superhard carbon allotrope

Heng Liu(刘恒), Qing-Yang Fan(樊庆扬)†, Fang Yang(杨放), Xin-Hai Yu(于新海), Wei Zhang(张伟), and Si-Ning Yun(云斯宁)‡
Chin. Phys. B, 2020, 29 (**10**): 106102. DOI: 10.1088/1674-1056/ab9c01

Fundamental band gap and alignment of two-dimensional semiconductors explored by machine learning

Zhen Zhu(朱震), Baojuan Dong(董宝娟), Huaihong Guo(郭怀红), Teng Yang(杨腾), Zhidong Zhang(张志东)
Chin. Phys. B, 2020, 29 (**4**): 046101. DOI: 10.1088/1674-1056/ab75d5

Structural, mechanical, and electronic properties of 25 kinds of *III*-*V* binary monolayers:A computational study with first-principles calculation

Xue-Fei Liu(刘雪飞), Zi-Jiang Luo(罗子江), Xun Zhou(周勋), Jie-Min Wei(魏节敏), Yi Wang(王一), Xiang Guo(郭祥), Bing Lv(吕兵), Zhao Ding(丁召)
Chin. Phys. B, 2019, 28 (**8**): 086105. DOI: 10.1088/1674-1056/28/8/086105

Quantum density functional theory studies of structural, elastic, and opto-electronic properties of $ZMoO_3$ (Z=Ba and Sr) under pressure

Saad Tariq, A A Mubarak, Saher Saad, M Imran Jamil, S M Sohail Gilani
Chin. Phys. B, 2019, 28 (**6**): 066101. DOI: 10.1088/1674-1056/28/6/066101

Effect of structural vacancies on lattice vibration, mechanical, electronic, and thermodynamic properties of Cr_5BSi_3

Tian-Hui Dong(董天慧)[1], Xu-Dong Zhang(张旭东)[1,†], Lin-Mei Yang(杨林梅)[1], and Feng Wang(王峰)[2]

[1] *School of Science, Shenyang University of Technology, Shenyang* 110870, *China*
[2] *School of Materials Science and Engineering, Shenyang University of Technology, Shenyang* 110870, *China*

(Received 13 May 2021; revised manuscript received 30 June 2021; accepted manuscript online 7 July 2021)

In recent years, transition metal silicides have become the potential high temperature materials. The ternary silicide has attracted the attention of scientists and researchers. But their inherent brittle behaviors hinder their wide applications. In this work, we use the first-principles method to design four vacancy defects and discuss the effects of vacancy defects on the structural stability, mechanical properties, electronic and thermodynamic properties of hexagonal Cr_5BSi_3 silicide. The data of lattice vibration and thermodynamic parameters indicate that the Cr_5BSi_3 with different atomic vacancies can possess the structural stabilities. The different atomic vacancies change the mechanical properties and induce the Cr_5BSi_3 to implement the brittle-to-ductile transition. The shear deformation resistance and volume deformation resistance of Cr_5BSi_3 are weakened by different vacancy defects. But the brittleness behavior is remarkably improved. The structural stability and brittle-to-ductile transition of Cr_5BSi_3 with different vacancies are explored by the electronic structures. Moreover, the thermal parameters indicate that the Cr_5BSi_3 with vacancies exhibit different thermodynamic properties with temperature rising.

Keywords: vacancies in Cr_5BSi_3, brittle-to-ductile transition, electronic properties, thermodynamic properties

PACS: 61.43.Bn, 61.72.Bb, 61.72.jd, 62.20.–x **DOI:** 10.1088/1674-1056/ac11e2

1. Introduction

With the development of science and technology, many researchers have discovered that the transition metal silicides can be used as the sharp leading edges materials and high temperature reusable surface materials of hypersonic vehicles and surface coatings, and so on.[1–4] They have the excellent chemical and physical properties, such as high oxidation resistance, high creep resistance, high strength and high melting point.[5–10] Some ternary metal silicides were found and their physical properties were widely investigated.[11–15] Among these ternary silicides, Nowotny *et al*. synthesized the Cr_5BSi_3 experimentally and found that it possesses the hexagonal structure with $P63/mcm$ group.[15] Zhou *et al*. predicted the anisotropic properties and band structure of Cr_5BSi_3 by using the first-principles calculations.[16] The theoretical results indicated that the Cr_5BSi_3 silicide shows the brittle behavior. Generally speaking, vacancy defects, doping elements, dislocation slip, *etc*. can improve the brittle behavior for solid materials.[17–19] For the heat activation effect in high temperature environment, the vacancy has a significant effect on the mechanical properties of high temperature materials. It is necessary to explore the effects of vacancies on the physical properties for Cr_5BSi_3. In the present work, we design four vacancy models and investigated the influences of these vacancies on the physical properties for Cr_5BSi_3. The structural stabilities, mechanical properties, electronic structures and thermodynamic properties of Cr_5BSi_3 with various vacancies are comparatively studied by using the first-principles calculations.

2. Theoretical methods

The parent Cr_5Si_3B and the Cr_5Si_3B with various vacancies were all investigated by using the CASTEP code.[20] The electron–ion interaction was described by the ultrasoft pseudopotential.[21,22] The Perdew-Burke–Ernzerhof (PBE) functional under the generalized gradient approximation (GGA) approximation was used to treat the exchange–correlation functional.[23] The electronic configurations of Cr, B, Si atoms are $3p^6 3d^5 4s^2$, $2s^2 2p^1$, and $3s^2 3p^2$, respectively. The cutoff energy of 560 eV was set such that the convergence for each of the present models was ensured. The Brillouin-zone was sampled by using an $8\times8\times10$ k-points for integrations in reciprocal space. The Broyden–Fletcher–Goldfarb–Shanno (BFGS) minimization scheme, ionic Hellmann–Feynman force, maximum ionic displacement and stress were used for optimizing the structure.[24–26] The tolerance for geometry optimization is different: within -5×10^{-3} eV/atom for the total energy, within 0.04 eV/Å for maximum ionic Hellmann–Feynman force, within 6×10^{-3} Å for maximum ionic displacement, and within 0.05 GPa for maximum stress. The current settings ensured that the total energy converged to 1 meV/atom. Convergence tests indicated that the cutoff energy and k mesh in the present work were sufficient to guarantee the convergence of total energy and provide a proper prediction of the lattice

†Corresponding author. E-mail: zxdwfc@163.com

© 2022 Chinese Physical Society and IOP Publishing Ltd

parameters. The unit cell sizes and atomic positions were allowed to be fully relaxed without any constraints during geometry optimization.

According to the available literature,[15,16] the Cr_5BSi_3 crystallizes into a hexagonal Cr_5CuSn_3-type structure with *P6₃/mcm* space group.[27] In the crystal structures of Cr_5BSi_3, Cr1, Cr2, B, and Si atoms occupy the locations at the Wyckoff sites 6*g* (0.27, 0, 0.25), 4*d* (0.33, 0.67, 0), 2*b* (0, 0, 0), and 6*g* (0.62, 0, 0.25), respectively. There are 18 atoms inside the unit cell. According to the four different atomic positions, we designed four vacancy models: Cr_{-Va1}, Cr_{-Va2}, B_{-Va}, and Si_{-Va}. And the four different structural models of Cr_5BSi_3 are shown in Fig. 1. The structural stability depends on the thermodynamical and dynamical condition. Thus, the vacancy formation energy (E_f) for each of the four models was calculated to estimate the thermodynamical stability in Cr_5BSi_3 with the following expression:[28,29]

$$E_f = E_{va}^{total} - E_{perf}^{total} + n\mu_X, \tag{1}$$

where E_{perf}^{total} represents the total energy of perfect Cr_5BSi_3 and E_{va}^{total} denotes the total energy of Cr_5BSi_3 with vacancy defects, and μ_X (X = Cr, B and Si) is the chemical potential of each species. For the niobium-rich region, $\mu_{Cr} = E_{Cr}(bulk)$, $\mu_B = E_B(bulk)$, while for the silicon-rich region, $\mu_{Si} = E_{Si}(bulk)$. Note that $E_{Cr}(bulk)$, $E_B(bulk)$, and $E_{Si}(bulk)$ are the total energy of a Cr atom, a B atom, and an Si atom in a bulk Cr, B, and Si system, respectively.[30–35] Futhermore, the thermodynamic stability for each of the four models was determined by the value of formationenthalpy. The formation enthalpy of perfect Cr_5BSi_3 was calculated from Eq. (2) and the values of formation enthalpy of four vacancy models were calculated from Eq. (3):[35,36]

$$\Delta H = \frac{1}{x+y+z}\left(E_{perf}^{total}(Cr_xB_ySi_z) - xE_{total}(Cr) - yE_{total}(B) - zE_{total}(Si)\right), \tag{2}$$

$$\Delta H = \frac{1}{x+y+z}\left(E_{vacancy}^{total}(Cr_xB_ySi_z) - xE_{total}(Cr) - yE_{total}(B) - zE_{total}(Si)\right), \tag{3}$$

where ΔH is the formation enthalpy, E_{perf}^{total} represents the total energy of perfect Cr_5BSi_3, $E_{vacancy}^{total}$ denotes the total energy of Cr_5BSi_3 with vacancy defects, and $E_{total}(Cr)$, $E_{total}(B)$, $E_{total}(Si)$ refer to the total energy of the crystal of Cr, B, and Si elements, respectively. Moreover, the structural stability is also determined by the dynamical condition. The dynamical stability depends on the phonon frequency. If the solid material possesses the positive phonon frequency, it will possess the dynamical stability. In this work, the phonon dispersions were investigated using the finite displacement method with Phonon code. Moreover, some phonon-related thermodynamic properties were calculated in a quasi-harmonic approximation within the Phonon code.[37–41] The mechanical properties were determined by the elastic constants (C_{ij}), and elastic moduli.[42–44] The strain–stress method and Voigt–Reuss–Hill (VRH) method were used to calculate the elastic constants and elastic moduli.[45,46] According to the Hill's bulk modulus B_H and shear modulus G_H, we calculated the elastic hardness (H_V), Poisson's ratio (v), and Young's modulus E.[47,48]

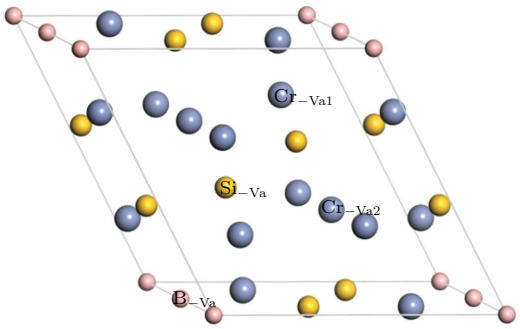


Fig. 1. Crystal structures of Cr_5BSi_3 with different vacancies.

3. Results and discussion

4. Structural stability of vacancy models

Table 1 shows the lattice parameters and thermodynamic parameters of four vacancy models and perfect Cr_5BSi_3 crystal. It is found that lattice constants of Cr_5BSi_3 approach to the experimental values,[15] which indicates that our computational method is reliable and feasible. As is well known, the positive vacancy formation energy (E_f) suggests that the vacancy model is thermodynamically stable.[35] As shown in Table 1, the values of vacancy formation energy E_f for four vacancy models are all positive, indicating that the Cr_5BSi_3 with four vacancies are thermodynamically stable. In Table 1, the values of formation enthalpy ΔH of perfect Cr_5BSi_3 and Cr_5BSi_3 with four vacancies are both negative, confirming that the Cr_5BSi_3 with various vacancies are thermodynamically stable. The Cr_{-Va1} vacancy has the best thermodynamic stability in these vacancies due to the most negative values of formationenthalpy. Furthermore, figure 2 displays the lattice vibration curves of parent Cr_5BSi_3 and four vacancy models. The parent Cr_5BSi_3 and Cr_5BSi_3 with various vacancies exhibit the dynamical stabilities because the parent Cr_5BSi_3 and Cr_5BSi_3 with various vacancies have no imaginary phonon frequencies in the whole regions.[49] It can be found from Table 1 that lattice constants of Cr_5BSi_3 with vacancies are smaller than those of the perfect Cr_5BSi_3 compound. In Fig. 1, each B atom is surrounded by six Cr1 atoms. And Cr2 atom occupies the center formed by three adjacent $BCr1_6$ octahedra. Additionally, the coplanar $BCr1_6$ octahedra are interleaved by Si layers along the c axis. The structural stability of Cr_5BSi_3 stems from the bond state formed by the hybridization among Cr, B, and Si atoms within the stacked layered structure. The removal of Cr, B, and Si atoms can cause lattice to shrink, which indicates that the removal of atoms enhances the atomic interaction among the nearby atoms.

Table 1. Calculated values of lattice parameters a, b, and c (in unit Å), vacancy formation energy E_f (in unit eV), and formation enthalpy ΔH (in unit eV) of Cr_5BSi_3 with four different vacancies.

Compound	Method	a (Å)	b (Å)	c (Å)	E_f (eV)	ΔH (eV)
Cr_5Si_3B	GGA	7.034	7.034	4.740		0.902
	Exp.[a]	7.060	7.060	4.730		
	Theor.[b]	7.0306	7.0306	4.7326		
Cr_{-Va1}	GGA	6.966	6.967	4.688	0.779	0.894
Cr_{-Va2}	GGA	6.934	6.933	4.732	0.761	0.889
B_{-Va}	GGA	6.981	6.981	4.717	0.736	0.878
Si_{-Va}	GGA	7.020	7.022	4.679	0.741	0.881

[a]Ref. [15], [b]Ref. [16].

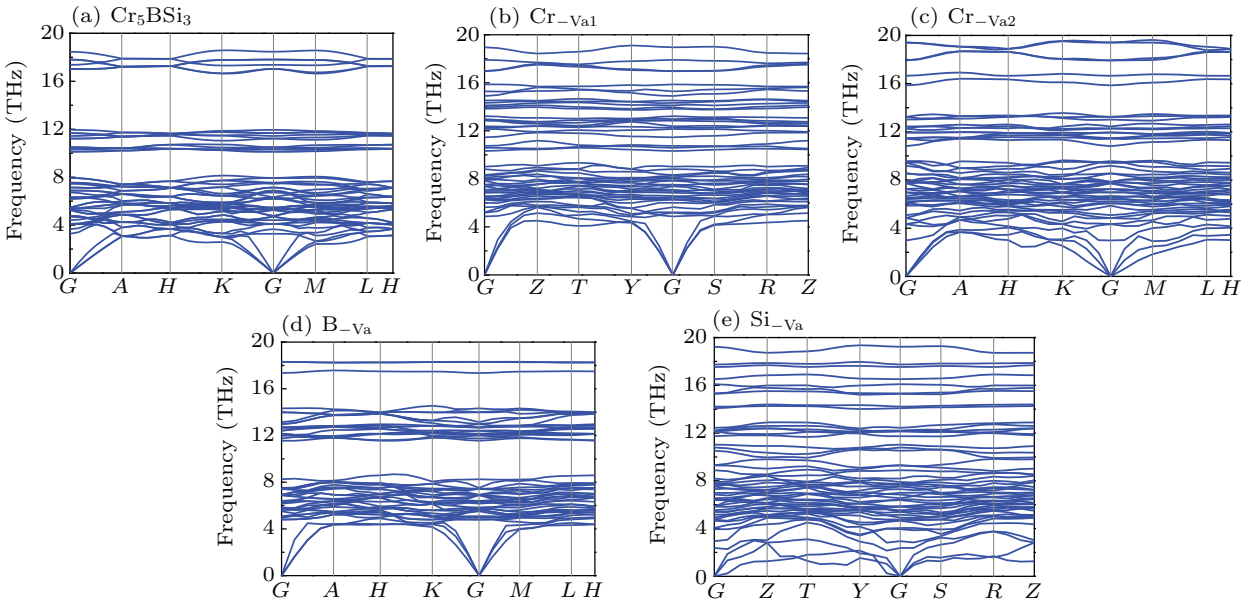


Fig. 2. Phonon dispersion curves of (a) parent Cr_5BSi_3 and Cr_5BSi_3 with different vacancies: (b) Cr_{-Va1}, (c) Cr_{-Va2}, (d) B_{-Va}, and (e) Si_{-Va}.

4.1. Mechanical properties

Table 2 presents the elastic constants C_{ij}s, elastic moduli and the related mechanical quantities of four models, together with the corresponding parameters of perfect Cr_5BSi_3. In Table 2, the calculated results are close to the available results.[16] The calculated elastic constants of Cr_5BSi_3 with various vacancies satisfy the Born criteria, indicating that they are mechanicallystable.[50,51] The deformation resistance along the a axis and the c axis are determined by the elastic constants C_{11} and C_{33}, respectively. A larger elastic constant C_{11} or C_{33} corresponds to a better deformation resistance. In the present work, the elastic constant C_{11} of the parent Cr_5BSi_3 is larger than the values of corresponding elastic constant C_{11} of two Cr_{-Va} vacancies and Si_{-Va} vacancy, confirming that the removal of these atoms can weaken the deformation resistance along the a axis. Meanwhile, elastic constant C_{33} of Cr_{-Va2} vacancy is smaller than that of the parent Cr_5BSi_3, illustrating that the presence of Cr_{-Va2} vacancy can enhance the deformation resistance along the c axis of parent Cr_5BSi_3. Furthermore, a larger elastic constant C_{44} implies a higher shear resistance.[52] As listed in Table 2, the elastic constant C_{44} of Si_{-Va} model is 100.7 GPa, which is smaller than those of parent Cr_5BSi_3 and Cr_5BSi_3 with other vacancies. Namely, the removal of Si atom makes the shear resistance of Cr_5BSi_3 lower than those of the parent Cr_5BSi_3 and Cr_5BSi_3 with other vacancies models. Therefore, the removal of atoms can weaken the charge interaction and the local hybridization among atoms in the ground state.

From Table 2 it follows that the bulk modulus B and shear modulus G of the perfect Cr_5BSi_3 are 197.9 GPa and 128.1 GPa, respectively. The values of B and G of Cr_{-Va} model and B_{-Va} model are smaller than those of the parent Cr_5BSi_3, indicating that the presence of Cr_{-Va} model and B_{-Va} model can weaken the compression resistance and deformation resistance of Cr_5BSi_3. In addition, when Si atom is removed, the values of B and G for Si_{-Va} model are larger than those of the parent Cr_5BSi_3, confirming that the Cr_5BSi_3 with Si_{-Va} vacancy possesses the better volume deformation. The shear modulus of B_{-Va} model is 86.9 GPa and it is smaller than those of other vacancy models, illustrating that B_{-Va} model has a weaker deformation resistance than other vacancy models. Generally speaking, the smaller Young's modulus means the lower elastic stiffness. In Table 2, the Young's moduli

of Cr_5BSi_3 and Cr_5BSi_3 with four various models follow the order: Si_{-Va}>Cr_5BSi_3>Cr_{-Va2}>Cr_{-Va1}>B_{-Va}, which indicates that the Si_{-Va} model possesses the best elastic stiffness in the four vacancy models. Additionally, it can be concluded that the presence of Cr atom and B atom vacancies can weaken the elastic stiffness of the parent Cr_5BSi_3.

Table 2. Values of elastic constants C_{ij} (in unit GPa), bulk modulus B (in unit GPa), shear modulus G (in unit GPa), Young's modulus E (in unit GPa), B/G ratio, Poisson's ratio v, and Vickers hardness H_V (in unit GPa) of Cr_5BSi_3 with four different vacancies.

Compound	C_{11}	C_{12}	C_{13}	C_{33}	C_{44}	C_{66}	B	G	E	B/G	v	H_V
Cr_5BSi_3	372.9	118.4	122.1	314.7	142.6	127.2	217.9	132.8	336.1	1.64	0.234	17.6
Theor.[a]	388	121	132	324	148	143	223	138	343	1.615	.243	
Cr_{-Va1}	350.5	129.4	98.2	366.4	132.8	98.5	193.5	115.7	289.4	1.67	0.251	14.7
Cr_{-Va2}	365.2	114.4	122.7	294.6	137.7	125.5	192.8	123.4	305.1	1.56	0.236	16.8
B_{-Va}	391.3	124.3	112.9	365.9	130.7	134.4	184.0	86.9	225.2	2.12	0.296	8.3
Si_{-Va}	278.8	152.9	110.5	348.1	100.7	79.0	205.8	132.5	327.3	1.55	0.235	17.8

[a]Ref. [16].

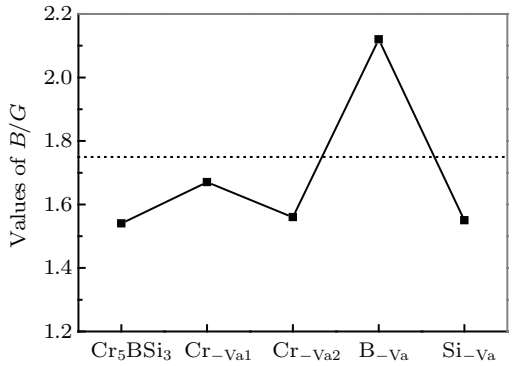


Fig. 3. Curves of B/G ratio of parent Cr_5BSi_3 and Cr_5BSi_3 with different vacancies.

The values of hardness H_V of Cr_5BSi_3 and Cr_5BSi_3 with different vacancies are listed in Table 2. The intrinsic hardness of the parent Cr_5BSi_3 is 17.6 GPa. The hardness H_V of the Cr_{-Va} model and Si_{-Va} model are slightly different from that of Cr_5BSi_3. The hardness H_V of B_{-Va} model is obviously smaller than that of Cr_5BSi_3. This result suggests that the removal of B atom strongly reduces the hardness of Cr_5BSi_3. The brittle/ductile behavior is a significant parameter of solid material. The B/G ratio and Poisson's ratio v can be used to assess the brittle or ductile behavior according to the Pugh rule.[53,54] The critical value of B/G and Poisson's ratio v are 1.75 and 0.26, respectively. If the values are less than 1.75 and 0.26, the solid material will be a brittle material. It is obviously found that B/G ratio of the parent Cr_5BSi_3 is less than 1.75 in Fig. 3, indicating that the parent Cr_5BSi_3 exhibits the brittle behavior.[16] The Cr_{-Va} model and Si_{-Va} model exhibit a slightly larger B/G ratio than the parent Cr_5BSi_3. However, the B/G ratio of B_{-Va} model is larger than 1.75. Namely, the Cr_5BSi_3 with B_{-Va} is a ductile material and the other vacancies improve the brittleness of Cr_5BSi_3, the variation of which is the same tendency as the variation of hardness. In Table 2, the Poisson's ratio v of the parent Cr_5BSi_3 is 0.234 GPa, which is less than 0.26, indicating that the Cr_5BSi_3 is a brittle material. Obviously, the Cr_5BSi_3 with B_{-Va} vacancy is ductile, and the Cr_{-Va} model and Si_{-Va} model are less brittle than the Cr_5BSi_3, which corresponds to the same variation with B/G ratio. The results indicate that the vacancy models improve the brittle behaviors of Cr_5BSi_3 and the B_{-Va} vacancy gives rise to the brittle-to-ductile behavior transition.

4.2. Electronic properties

To further investigate the mechanism of electronic properties, the total and partial density of states for the Cr_5BSi_3 with various vacancies are shown in Fig. 4. The black vertical dotted lines in the graphs denote the Fermi level E_F. It is found that there are no energy gaps appearing near the Fermi level E_F, which indicates that the Cr_5BSi_3 exhibits the metallic behavior. As shown in Fig. 4(a), the density of states (DOS) of Cr_5BSi_3 is mainly composed of the Cr-3d, B-2s, 2p, and Si-3s, 3p orbital states. For the different contributions of Cr, B, and Si electronic states, the localized hybridization between electronic states forms the Cr–B bond, Cr–Si bond, and B–Si bond. The B-2p state penetrates into the B-2s state at −6.35 eV, implying that the electrons transfer from B-2s to B-2p state. The Cr-3d state and Cr-4s state cross the Cr-3p for −8.59 eV and −6.38 eV, respectively, which indicates that the electrons transfer between Cr-3d, Cr-4s, and Cr-3p states. The Si-3p state passes through the Si-3s state at −6.82 eV, which means the formation of Si–Si bonds. It can be seen from the figure, the localized hybridization between the Cr-3d state and the B-2p state in Cr_5BSi_3 is strong, which results in the strong electronic interaction between Cr and B atoms. The density of states (DOS) for Cr_5BSi_3 with various vacancies is slightly different from that of the parent Cr_5BSi_3. The structural stability can be exhibited by the number of bonding electrons at Fermi level, the smaller the value of the number, the more stable the structure is.[55,56] The N (E_F) values of the Cr_5BSi_3 with four vacancies and the parent Cr_5BSi_3 follow the order: Cr_{-Va2}<Cr_{-Va1}<Cr_5BSi_3<Si_{-Va}<B_{-Va}, which illustrates that the presence of Cr_{-Va} vacancies can enhance the structural stability of parent Cr_5BSi_3. On the contrary, the removal of B and Si atoms makes the parent Cr_5BSi_3 less stable. The valleys near the Fermi level of Cr_5BSi_3 with Cr vacancies are shallower than those of the parent Cr_5BSi_3, which means

the existence of Cr vacancies can enhance the electronic interaction and reflect the better deformation resistance of the Cr vacancies.[57] In Fig. 4(e), the valleys near Fermi level almost disappear, which illustrates that the presence of Si_{-Va} vacancy causes more charges to transfer to Fermi level. Namely, the localized hybridization between B atoms and Cr atoms is promoted, which makes the bond length of Cr–B shorter and the bond strength stronger.

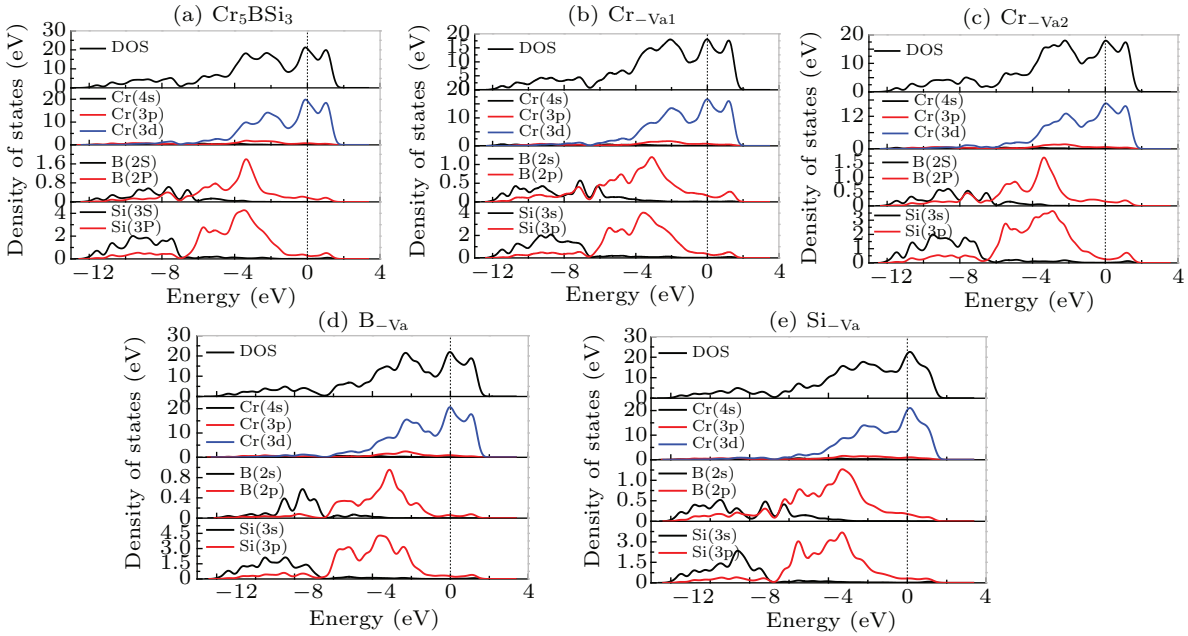


Fig. 4. Total and partial DOSs of (a) parent Cr_5BSi_3 and Cr_5BSi_3 with different vacancies: (b) Cr_{-Va1}, (c) Cr_{-Va2}, (d) B_{-Va}, and (e) Si_{-Va}.

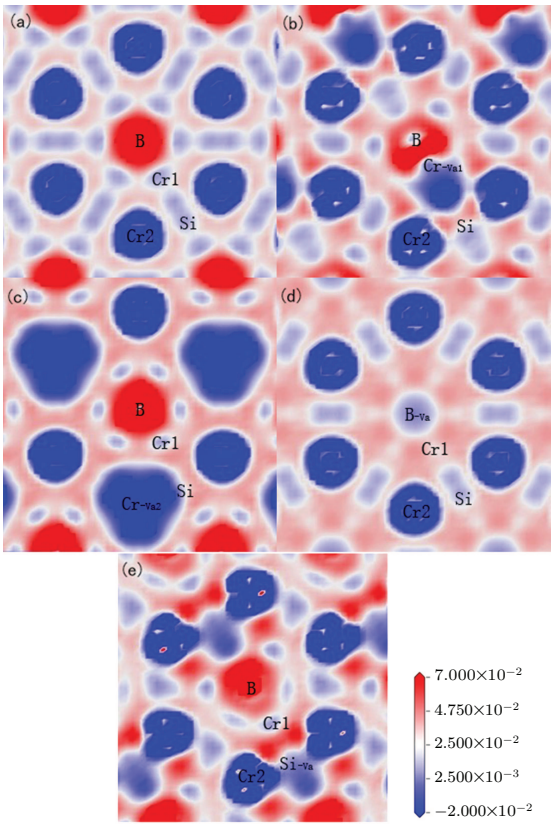


Fig. 5. Plots of electron density difference for (a) parent Cr_5BSi_3 and Cr_5BSi_3 with different vacancies: (b) Cr_{-Va1}, (c) Cr_{-Va2}, (d) B_{-Va}, and (e) Si_{-Va}.

The differences in electron density between the parent Cr_5BSi_3 and the Cr_5BSi_3 with four vacancies on (001) plane are plotted in Fig. 5. In eachpanel, the difference in electron density is in a range from -0.02 e/Å^3 to 0.07 e/Å^3. And the blue color and the red color denote the maximum and minimum accumulation of electrons, respectively. The light blue regions refer to the neutral regions and there is no charge transfer in these regions. Comparing with the color bar, it can be found from Fig. 5(a) that there are many electrons accumulating between nearby Cr1 and B atoms, illustrating that there exist the Cr1–B–Cr1 bond chains in the parent Cr_5BSi_3. There is no electron accumulation between Cr1 atom and Si atom appearing in Fig. 5(a), indicating that the electrons are delocalized between Cr atom and Si atom. However, there is no obvious transformation between the inter-layer B atoms, indicating that the weak B–B interaction appears. Furthermore, the electrons between the neighboring Cr2 atoms are delocalized, and so are the nearby Si atoms, which indicates that Cr2–Cr2 bonds and Si–Si bonds are both metallic bonds. The presence of vacancies can influence the electron accumulation, which changes the state of bond and mechanical properties of the parent Cr_5BSi_3. From Fig. 5(b), the Cr_{-Va1} vacancy reduces the strength of Cr1–B bond and Cr1–Si bond, which reduces the resistance of deformation on the (001) plane. The Cr_{-Va2} vacancy reduces the localized hybridization between nearby Cr2 atoms. Particularly, when B atoms are removed, the electrons between Cr1 atom and B atom become more delocalized, meanwhile the hybridization between Cr1 atom and Si atom becomes stronger. The weak localized hybridization im-

proves the brittle behavior of the parent Cr_5BSi_3. The Cr1–Si bonds are clear away in Fig. 5(e), indicating that the presence of Si_{-Va} vacancy reduces the localized hybridization between Cr1 atoms and Si atoms.

4.3. Thermodynamic properties

As is well known, the thermal response of material can be estimated by the thermodynamic properties. To estimate the thermodynamic properties of the Cr_5BSi_3 with four vacancies, we use the Phonon code to explore their thermodynamic properties. Figures 6 and 7 show the thermodynamic parameters of Cr_5BSi_3 with four vacancies at different temperatures. Figure 6 shows the curves of calculated values of heat capacity at constant volume C_V versus temperature for Cr_5BSi_3 with four vacancies and the parent Cr_5BSi_3. It is found that the values of heat capacity C_V of Cr_5BSi_3 with four vacancies and the parent Cr_5BSi_3 follow the Debye T^3 law in low temperature area and are close to the Dulong–Petit limit in high temperature area.[58,59] The values of C_V for Cr_5BSi_3 with various vacancies are smaller than the value of C_V of parent Cr_5BSi_3, which indicates that the removal of Cr, B, and Si atoms reduce the value of C_V of the parent Cr_5BSi_3.

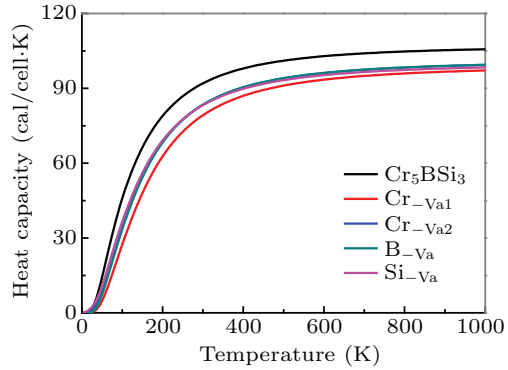


Fig. 6. Temperature-dependent heat capacity (C_V) curves of parent Cr_5BSi_3 and Cr_5BSi_3 with different vacancies.

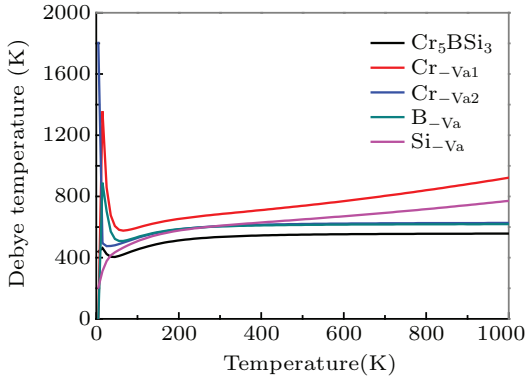


Fig. 7. Curves of Debye temperature (Θ_D) *versus* temperature of parent Cr_5BSi_3 and Cr_5BSi_3 with different vacancies.

Figure 7 shows the curves of Debye temperature *versus* temperatue of Cr_5BSi_3 with various vacancies. It is obvious that Debye temperatures of Cr_5BSi_3 with various vacancies and the parent Cr_5BSi_3 increase rapidly in low temperature area and are close to the fixed values in high temperature area. The Debye temperatures of Cr_5BSi_3 with various vacancies in high temperature area are much larger than the Debye temperature of the parent Cr_5BSi_3, indicating that the existence of these vacancies increases the thermal stability of the parent Cr_5BSi_3. The Debye temperature of the Cr_5BSi_3 with Cr_{-Va1} vacancy is much bigger than those of other compounds, which illustrates that the Cr_5BSi_3 with Cr_{-Va1} vacancy shows the better thermal stability than other compounds in the elevated temperature region.

5. Conclusions

We use the first-principles calculations to explore the effects of vacancies on the structural stability, electronic and mechanical properties of Cr_5BSi_3. The conclusions are as follows.

(i) Theremoval of Cr, B, and Si atoms result in lattice shrinkage. Their vacancy formation enthalpy values are all smaller than zero, indicating that these vacancy structures are thermodynamically stable. The Cr_{-Va1} model is more stable than other vacancy models. The lattice vibration indicates that the Cr_5BSi_3 with various vacancies are dynamically stable.

(ii) The elastic modulus of Cr_5BSi_3 with Cr_{-Va} vacancies and B_{-Va} vacancies are smaller than that of Cr_5BSi_3, demonstrating that these vacancies weaken the hardness and deformation resistance of Cr_5BSi_3. The Poisson's ratio v and B/G indicate that Cr_5BSi_3 with B_{-Va} vacancy induces the brittle-to-ductile behavior transition.

(iii) The electronic properties explain the mechanism of an effect of structural vacancies on the physical properties of Cr_5BSi_3.

(iv) The values of thermal parameters indicate that the Cr_5BSi_3 with four vacancies present different thermodynamic properties with the increase of temperature.

Acknowledgement

Project supported by the Natural Science Foundation of Liaoning Province, China (Grant No. 2019JH/30100019).

References

[1] Opela M M, Talmy I G and Zaykoski J A 2004 *J. Mater. Sci.* **39** 5887
[2] Wie D M, Drewry D G, King D E and Hudson C M 2004 *J. Mater. Sci.* **39** 5915
[3] Corral E L and Loehman R E 2008 *J. Am. Ceram. Soc.* **91** 1495
[4] Blum Y D, Marschall J, Hui D and Young S 2008 *J. Am. Ceram. Soc.* **91** 1453
[5] Roger J, Babizhetskyy V, Cordier S, Bauer J, Hiebl K, Le Polles L, Ashbrook S E, Halet J F and Guerin R 2005 *J. Solid State Chem.* **178** 1851
[6] Tao X, Jund P, Colinet C and Tedenac J C 2009 *Phys. Rev. B* **80** 104103
[7] Shugani M, Aynyas M and Sanyal S P 2015 *Indian J. Pure Appl. Phys.* **51** 104
[8] Aydin S, Tatar A and Ciftci Y O 2016 *Solid State Sci.* **53** 44

[9] Pan Y and Guan W M 2017 *Phys. Chem. Chem. Phys.* **19** 19427
[10] Pan Y and Guan W M 2019 *Ceram. Int.* **45** 15649
[11] Wang D Z, Hu Q W and Zeng X Y 2014 *J. Alloys Compd.* **588** 502
[12] Cai G M, Zheng F, Yi D Q, Chen H M, Zhou S X, Long Z H and Jin Z P 2010 *J. Alloys Compd.* **494** 148
[13] Müller C, Hasemann G, Regenberg M, Betke U and Krüger M 2020 *Materials* **13** 2100
[14] Pan Y, Guan W M and Li Y Q 2018 *Phys. Chem. Chem. Phys.* **20** 15863
[15] Nowotny H, Piegger E, Kieffer R and Benesovsky F 1958 *Monatsh. Chem.* **89** 611 (in German)
[16] Zhou Y C, Xiang H M, Dai F Z and Feng Z 2018 *J. Mater. Sci. Technol.* **34** 1441
[17] Pan Y 2019 *J. Electron. Mater.* **48** 5154
[18] Chen J Y, Zhang X D, Li D Z, Liu C, Ma H, Ying C H and Wang F 2020 *Ceram. Int.* **46** 4595
[19] Sun L, Wang W, Liu C, Lv D, Gao Z Y and Xu B H 2021 *Superlattices Microstruct.* **149** 106775
[20] Segall M D, Lindan P J D, Probert M J, Pickard C J, Hasnip P J, Clark S J and Payne M C 2002 *J. Phys. Math.* **14** 2717
[21] Vanderbilt D 1990 *Phys. Rev. B* **41** 7892
[22] Kresse G and Joubert D 1999 *Phys. Rev. B* **59** 758
[23] Prfrommer B G, Côté M, Loiue S G and Cohen M L 1997 *J. Comput. Phys.* **131** 233
[24] Wang P, Zhang N C and Jiang C 2020 *Chin. Phys. B* **29** 076201
[25] Noor N A, Mushahid N and Khan A 2020 *Chin. Phys. B* **29** 097101
[26] Wen M, Xie X and Dong H 2020 *Chin. Phys. B* **29** 078103
[27] Rieger W and Parthé E 1968 *Acta Crystallogr. Sect. B: Struct. Sci.* **24** 456
[28] Chen J Y, Zhang X D, Ying C H, Ma H, Wang F and Guo H 2020 *Ceram. Int.* **46** 10992
[29] Wang W, Sun L, Li Q, Lv D, Gao Z Y and Huang T 2021 *J. Magn. Magn. Mater.* **527** 167692
[30] Zhu X Y, Gao X, Song H, Han G and Lin D 2017 *Mater. Des.* **119** 30
[31] Pan Y, Zhang J, Jin C and Chen X 2016 *Mater. Des.* **108** 13
[32] Pan Y, Chen S and Lin Y 2017 *Int. J. Mod. Phys. B* **31** 1750096
[33] Yao J, Lin Y, Lin N and Le S 2012 *Physica B* **407** 3888
[34] Feng L, Su J and Liu Z 2014 *J. Alloys Compd.* **613** 122
[35] Freysoldt C, Grabowski B, Hickel T and Neugebauer 2014 *J Rev. Mod. Phys.* **86** 253
[36] Khyzhun O Y, Bekenev V L, Denysyuk N M, Isaenko L I, Yelisseyev A P, Goloshumova A A and Tarasova A Y 2019 *J. Electron. Mater.* **48** 3059
[37] Pu D L and Pan Y 2021 *Ceram. Int.* **47** 2311
[38] Wang W X, Jiang Z Y and Lin Y M 2020 *Chin. Phys. B* **29** 076101
[39] Chen J Y, Zhang X D, Yang L M and Wang F 2021 *Commun. Theor. Phys.* **73** 045702
[40] Wu Y, Bao L, Wang X, Wang Y, Peng M and Duan Y 2020 *Mater. Today Commun.* **25** 101410
[41] Hermet P, Khalil M, Viennois R, Beaudhuin M, Bourgogne D and Ravot D 2015 *RSC Adv.* **5** 19106
[42] He C, Zhang M, Li T T and Zhang W X 2020 *J. Mater. Chem. C* **8** 6542
[43] Zhou Z, Zhou X and Zhang K 2016 *Comput. Mater. Sci.* **113** 98
[44] He C, Zhang M, Li T T and Zhang W X 2020 *Appl. Surf. Sci.* **505** 144619
[45] Shang S, Wang Y and Liu Z K 2007 *Appl. Phys. Lett.* **90** 101909
[46] Wang Y, Wu Y, Wang X, Duan Y and Peng M 2021 *J. Phy. Chem. Solids* **151** 109925
[47] Hill R 1952 *Proc. Phys. Soc.* **65** 349
[48] Wang X, Bao L, Wang Y, Wu Y, Duan Y and Peng M 2021 *Mater. Today Commun.* **26** 101723
[49] He C, Zhang M, Li T T and Zhang W X 2020 *J. Mater. Chem. C* **8** 6542
[50] Mouhat F and Coudert F X 2014 *Phys. Rev. B* **90** 224104
[51] Wu Y, Wang X, Wang Y, Duan Y and Peng M 2021 *Opt. Mater.* **114** 110963
[52] Grimvall G 1999 *Thermo Physical Properties of Materials* (Amsterdam: North Holland)
[53] Pugh S F 1954 *Philos. Mag.* **45** 823
[54] Lewandowski J J, Wang W H and Greer A L 2005 *Philos. Mag. Lett.* **85** 77
[55] Li T T, He C and Zhang W X 2021 *J. Energy Chem.* **52** 121
[56] Li T T, He C and Zhang W X 2020 *Energy Storage Mater.* **25** 866
[57] He C, Zhang M and Zhang W X 2019 *Solid State Commun.* **303** 113736
[58] Kittel C 1996 *Introduction to Solid State Physics* (New York: Wiley)
[59] Duan Y, Wang Y, Peng M and Wang K 2021 *Mater. Today Commun.* **26** 101991